

Structural Modifications in Ion-Implanted Diamond

F. Bosia^{1,2}, S. Lagomarsino³, A. Lo Giudice^{4,5}, P. Olivero^{4,5}, F. Picollo^{4,5}, S. Sciortino³,
A. Sordini⁶, M. Vannoni⁶, E. Vittone^{4,5}, H. Wang^{4,5}

¹ *Theoretical Physics Department, University of Torino, Torino, Italy.*

² *INFN, Sezione di Torino, Torino, Italy.* ³ *Department of Energetics, University of Firenze, Firenze, Italy.*

⁴ *Experimental Physics Department and NIS Centre of Excellence, University of Torino, Torino, Italy.*

⁵ *INFN, Laboratori Nazionali di Legnaro, Legnaro (Padova), Italy.* ⁶ *Istituto Nazionale di Ottica, CNR, Arcetri (Firenze), Italy.*

INTRODUCTION

We present experimental results and numerical Finite Element analysis to describe the structural modification occurring in diamond when subjected to MeV ion implantation. Numerical predictions are compared to experimental data for MeV helium implantations performed at the scanning ion microbeam line of the AN2000 accelerator. Swelling values are measured with white light interferometric profilometry. Simulations are based on a model which accounts for the through-the-thickness variation of mechanical parameters in the material, as a function of ion fluence.

EXPERIMENTAL

Ion implantation was performed on artificial single crystal diamonds that were produced with “high pressure high temperature” (HPHT) technique by Sumitomo. The samples are cut along the 100 crystal direction and usually consist of different growth sectors. Their size is $3 \times 3 \times 1.5 \text{ mm}^3$, and the two opposite large faces are optically polished.

The samples were implanted in frontal geometry in a broad range of fluences with 1.8 MeV He⁺ ions at the ion microbeam line of the AN2000 accelerator of the INFN Legnaro National Laboratories. In order to achieve a uniform fluence delivery in the implantation process, $\sim 125 \times 125 \text{ }\mu\text{m}^2$ square areas were implanted by raster scanning an ion beam with size of 1-10 μm . The implantation fluence was controlled in real time by monitoring the x-ray yield from a thin metal layer evaporated on the sample surface. The implantations were performed at room temperature, with ion currents of $\sim 1 \text{ nA}$. In these conditions, implantations in the fluence ranges of $10^{15} - 10^{17} \text{ cm}^{-2}$ could be performed in times varying from few minutes to ~ 1 hour.

Surface swelling data were acquired at the Interferometry laboratories of the Istituto Nazionale di Ottica Applicata (INOA) with a Zygo NewView 6000 system, which exploits white light interferometry to provide detailed, non contact measurements of 3-D profiles. A vertical resolution of 0.1 nm was achieved over a lateral range up to 150 μm , while lateral resolution varied from 4.6 μm up to 0.6 μm , depending on the objective.

Figure 1 illustrates an example of a measured swelling profile from an area of approximately $110 \times 170 \text{ }\mu\text{m}^2$ implanted at a fluence of $3.67 \cdot 10^{16} \text{ cm}^{-2}$. The average swelling in the central region of this area is about 100 nm.

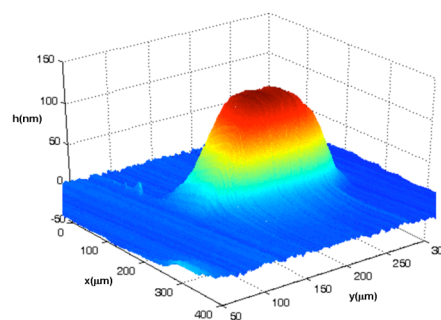


Fig. 1. Experimentally measured swelling h for a 1.8 MeV He⁺ implantation ($F=3.67 \cdot 10^{16} \text{ cm}^{-2}$) using the profilometry technique based on white light interferometry.

MODELING

A simple phenomenological model was developed that describes the density variation in diamond due to modifications in the crystal lattice during ion implantation. With the “SRIM - The Stopping and Range of Ions in Matter” (SRIM) Monte Carlo simulation code [1] it is possible to estimate the profile of the linear density of vacancies $\lambda(z)$, if no saturation effects are taken into account. It is expected that the formation of vacancies and interstitials leads to an amorphization of the material, i.e. a transition from the density of diamond ($\rho_d = 3.515 \text{ g cm}^{-3}$) to that of amorphous carbon ($\rho_{aC} \approx 1.557 \text{ g cm}^{-3}$). The greater the damage density, the smaller the density of the damaged diamond should become, with saturation towards the lower bound value of ρ_{aC} . As mentioned above, this saturation is not predicted by SRIM Monte Carlo code, in which the interaction of each single ion with the pristine crystalline structure is simulated and no cumulative damage effects are taken into account.

We developed a model that predicts non-linear damage saturation effects, which was derived from the assumption that the recombination probability for a vacancy in a damage cascade is proportional to the vacancy density [2]. On the basis of such model, the density ρ of the damaged

material at a given depth z for a given implantation fluence F is given by:

$$\rho(F, z) = \rho_d - (\rho_d - \rho_{ac}) \cdot \left(1 - e^{-\frac{F\lambda(z)}{\alpha}}\right) \quad (1)$$

where ρ_d is the density of diamond, ρ_{ac} is the saturation density of amorphous carbon, and α expresses the critical vacancy density at which all additional vacancies recombine with existing interstitial atoms in the damaged material.

The expected density variation as a function of depth z and fluence F is shown figure 2 in the fluence range $5 \cdot 10^{15} - 5 \cdot 10^{17} \text{ cm}^{-2}$, for $\alpha = 1.1 \cdot 10^{23} \text{ cm}^{-3}$.

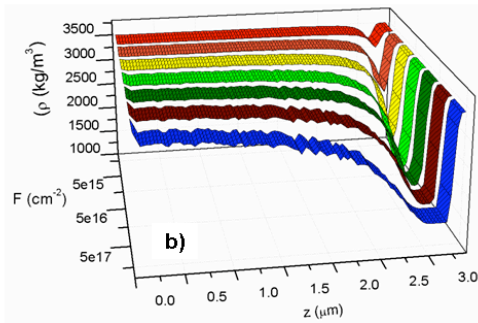


Fig. 2. Density variation of damaged diamond as a function of depth z and fluence F for a 1.8 MeV He^+ implantation ($\alpha = 1.1 \cdot 10^{23} \text{ cm}^{-3}$).

NUMERICAL SIMULATIONS AND RESULTS

Finite Element Method (FEM) simulations were performed with the commercial software COMSOL Multiphysics [3] by imposing a constrained isotropic volume expansion in the damaged diamond substrate, which is proportional to the local density variation, as evaluated in the above-mentioned model. The analytical expression of Eq. (1) is used, together with the damage profile $\lambda(z)$ resulting from SRIM simulations for 1.8 MeV He^+ in diamond, with atom displacement energy set to 50 eV [4]. The mechanical properties of diamond and amorphous carbon are $\rho_d = 3.515 \text{ g}\cdot\text{cm}^{-3}$, $E_d = 1144.6 \text{ GPa}$, $\nu_d = 0.2$ and $\rho_{ac} = 1.557 \text{ g}\cdot\text{cm}^{-3}$, $E_{ac} = 21.38 \text{ GPa}$, $\nu_{ac} = 0.184$, respectively [5].

Figure 3 shows an example of the deformation profile evaluated by FEM calculations relevant to the same irradiation conditions of figure 1 and assuming $\alpha = 1.1 \cdot 10^{23} \text{ cm}^{-3}$. As visible from the comparison of figures 1 and 3, the result of the numeric calculation is in excellent agreement with experimental results.

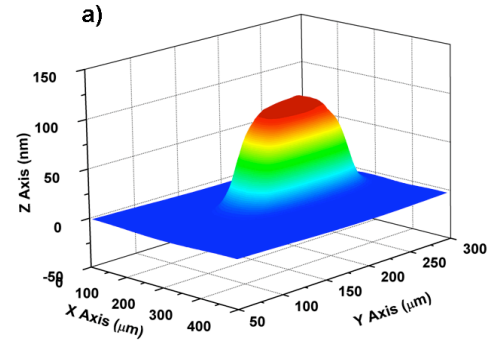


Fig. 3. FEM simulation swelling results for 1.8 MeV He^+ implantations with $F = 3.67 \cdot 10^{16} \text{ cm}^{-2}$ and $\alpha = 1.1 \cdot 10^{23} \text{ cm}^{-3}$.

Numerical FEM simulations were carried out by varying the parameter α to obtain the best agreement with experimental data. The “swelling vs fluence” plot in figure 4 shows experimental and numerical values for implantations at various fluences. The best fit is obtained for $\alpha = 0.44 \cdot 10^{23} \text{ cm}^{-3}$.

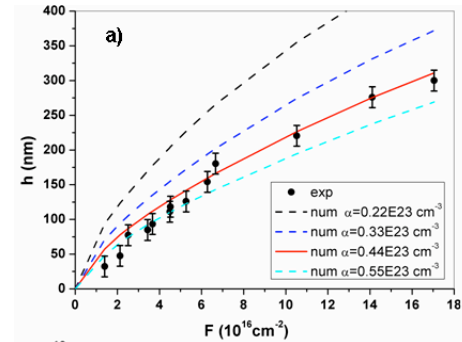


Fig. 4. Experimental (“exp”) and numerical (“num”) swelling values h vs. fluence F for 1.8 MeV He^+ ions.

CONCLUSIONS

The results reported in this paper prove that the FEM numerical analysis can significantly contribute to the quantitative interpretation of the structural damage mechanisms in ion-implanted diamond, and provides encouraging insight for further in-depth analysis and systematic studies at higher implantation fluences [6].

-
- [1] A. Ziegler, Littmark, U., (Ed.), The Stopping and Range of Ions in Solids, Pergamon, New York, 1985.
 - [2] J. F. Prins et al., Phys. Rev. B 34 (1986) 8870.
 - [3] COMSOL Multiphysics, <http://www.comsol.com/>.
 - [4] W. Wu et al., Phys. Rev. B 49 (1994) 3030.
 - [5] Y. X. Wei et al., Phys. Rev. B 72 (2005) 012203.
 - [6] F. Bosia et al., submitted to Nucl. Instr. and Methods B.